

Available online at [www.sciencedirect.com](http://www.sciencedirect.com)**ScienceDirect**

Energy Procedia 74 (2015) 1517 – 1524

Energy

**Procedia**

International Conference on Technologies and Materials for Renewable Energy, Environment and Sustainability, TMREES15

## Simulation and modeling of structural stability, electronic structure and optical properties of ZnO

H.I.Berrezoug<sup>a</sup>, A.E. Merad<sup>a</sup>, A. Zerga<sup>b</sup>, Z.Sari Hassoun<sup>c</sup>

<sup>a</sup>Theoretical Physics laboratory, physic Department, Abou-BakrBelkaid University, P.O. Box 119 13000 Tlemcen, Algeria

<sup>b</sup>URMER, physic Department, Abou-BakrBelkaid University, P.O. Box 119 13000 Tlemcen, Algeria

<sup>c</sup>MECACOMP, Mechanical Engineering Department, Abou-BakrBelkaid University, P.O. Box 119 13000 Tlemcen, Algeria

### Abstract

We propose a generalized gradient approximation simple and effective Engel-Vosko (GGA-EV) to calculate the structural, electronic, optical properties of ZnO phases, namely, wurtzite, zincblende structures using an implementation of the FP method (L) APW in the framework of the density functional theory (DFT). For Choosing a good exchange and correlation potential for effective treatment of the excited state properties such as electronic band structure is necessary density functional. To validate our approach, we compare the results to those obtained using the parameterized generalized gradient approximation of Perdew et al. (GGA-PBE). We calculated the band structure, density of states, dielectric function, reflectivity, refraction index and absorption coefficient. GGA-EV yielded a wider valence band and narrower d-band in comparison to GGA-PBE. Thus an improved the energy band gap that has been caused by repulsion between the states of Zn-d and O-p states which resulted a large separation by GGA-EV. Our calculations show that the edges of the optical absorption, refraction index and reflectivity for GGA-EV are better in comparison to GGA-PBE.

© 2015 Published by Elsevier Ltd. This is an open access article under the CC BY-NC-ND license (<http://creativecommons.org/licenses/by-nc-nd/4.0/>).

Peer-review under responsibility of the Euro-Mediterranean Institute for Sustainable Development (EUMISD)

*Keywords:* ZnO, the functional theory of density, the approach of the pseudo-potential, electronic properties, optical properties.

### 1. Introduction

Zinc oxide (ZnO) is a II–IV compound semiconductor with a wide direct band gap of 3,3eV [1] at room temperature and a free-exciton binding energy of 60meV [2]. ZnO has received considerable attention due to its applications such as: gas sensor devices [3], transparent electrodes [4], piezoelectric devices [5] and solar cells [6]. The theoretical and experimental efforts are huge in the study of the fundamental properties of existing materials

and new materials research. Theoretical studies are based on analytical models or computer simulations. The density functional theory (DFT) [7,8] is one of the most accurate and effective microscopic theories in computational materials science, which efficiently describes the ground-state physical properties of electronic systems using LDA-PW91 [8,9] or GGA-PBE [10,11] as the exchange-correlation energy functional. Calculations in these local (semi) approximations are sufficiently accurate and are helpful for interpretation of experimental data regarding ground-state properties [12]. However, DFT calculations with GGA-PBE do not properly interpret the excited-state properties, which results in underestimation of the band gap and over estimation of electron delocalization, particularly for systems with localized d and f electrons [13, 14]. In this approximation, the orbital-independent potential is taken in to account to calculate the Kohn–Sham energy gap, which is not comparable to the true gap, which is the ionization potential  $I$  minus the electron affinity  $A$  [12, 15, 16]. Another form of exchange correlation (XC) potential suggested by Engel and Vosko (GGA-EV) [17], yields better values for the electronic parameters [18–19]. In this study we investigated the use of GGA-EV for the band gap, electronic and optic properties of ZnO. The ZnO exists in hexagonal wurtzite WZ phase under ambient and can be obtained in zinc-blende (ZB) phase by growing it on a cubic substrate, which is important for controlled p-type conductivity [19, 20, 21,22,23]. Using the full potential linearized augmented plane-wave plus local orbital (FP-L (APW+lo)) method designed within the framework of DFT at the level of GGA-EV as the XC potential. We carried out a comprehensive study of the electronic and optical properties of ZnO in WZ and ZB phases to validate our approach, we compared the results obtained by GGA-EV with those obtained by GGA-PBE.

## 2. Method of calculation

The full-potential linear augmented plane waves plus local orbitals (FP-LAPW+lo) method was used to solve the Kohn–Sham equation within the density functional theory (DFT) [7, 8] formulation as employed in WIEN2k code [24]. The XC potential proposed by Engel and Vosko GGA- EV [17] was used to calculate electronic and optical properties of ZnO in WZ and ZB phases. To check the validity of this XC potential, calculations with GGA-PBE were also performed for comparison. The radius of muffin–tin (RMT) sphere values for Zn and O atoms were taken to be 1.85 and 1.64 a.u., respectively. The plane wave cut off parameters were  $RMT * K_{max} = 8.5$  (where  $K_{max}$  is the largest wave vector of the basis set). Regarding the number of k-points, 900 were used in these calculations, 120 k-points for wurtzite and 216 k-points for zinc-blende were used for the Brillouin zone integrations in the corresponding irreducible wedge. When the total energy convergence is less than  $10^{-4}$  Ry, the self-consistent calculation is considered to be stable.

## 3. Results and discussion

### 3.1. Structural properties

The calculated structure parameter, the other theoretical prediction and the experiment results are presented in Table 1. It is shown that our calculation agrees well with the other experimental and theoretical results.

We calculated the total energy as a function of the unit-cell volume around the equilibrium cell volume  $V_0$ . Fig. 1 shows the calculated total energies versus volume for the wurtzite and zinc blend phases of ZnO, or we notice that the wurtzite structure has the lowest energy which means it is more stable than the zinc-blend phase. The calculated total energies are fitted to an-empirical functional form (the third-order Murnaghan equation) [25] to obtain an analytical interpolation of our computed points from which to calculate derived structural properties.

Table 1. Structures parameters of ZnO.

ZnO	WZ	Other cal.	Exp.values	ZB	Exp.values
a (Å)	3.294	3.283[41], 3.292[27]	3.258[42], 3.25[23]	4.6227	4.47[33]
c (Å)	5.316	5.309[41], 5.292[27]	5.22[42], 5.204[23]	4.6227	
u	0.378	0.3786[41], 0.380[27]	0.382[42]		
B <sub>0</sub> (GPa)	129.135	131.6[41], 133.7[27]	181[42], 183[23]	129.228	
B'	4.424	4.2[41], 4.05[27]	4[42, 23]	4.43	

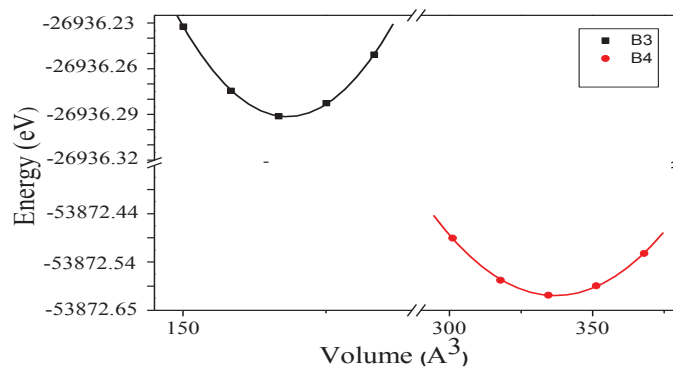


Fig. 1. The variation of the total energy as a function of the volume obtained for both zinc blende structure (B3), wurtzite (B4).

### 3.2. Electronic properties

To investigate the electronic and optical properties of ZnO, GGA-EV was used as the XC functional in DFT calculations. The electronic band structure of ZnO calculated for WZ and ZB phases within GGA-PBE and GGA-EV is shown in Fig.2. We note that the valence band maximum (VBM) and the conduction band minimum (CBM) are located at the  $\Gamma$  point in the Brillouin zone (BZ), resulting in a direct band gap. In the VB for WZ and ZB phases, the O-p orbital that exhibits  $t_{2g}$  symmetry is strongly hybridized to the Zn-d orbital with the same symmetry, resulting in a three-fold degenerate energy level at the  $\Gamma$  point in the BZ for ZB [28]. However, for WZ a two-fold degeneracy exists because of band folding along the [111]/ [0001] direction [27]. The band gap values computed according to GGA-PBE and GGA-EV are listed in Table2, along with experimental values and other theoretical calculations. It is evident from the data that the GGA-PBE band gap results are an excellent agreement with available theoretical results, but are underestimated in comparison to experimental data. This is because of the simpler form of these XC functional and their lack of flexibility in giving precise values of the XC energy and its charge derivative simultaneously. However, GGA-EV compensates this deficiency and reproduces better results for the band gap values. It has been successfully applied in several studies to investigate the electronic properties of solids and yields results that are comparable to experimental values because of a better choice of the XC potential in this approximation [18, 19].

Table 2. Band gap (eV) calculated for wurtzite and zinc-blend phases of ZnO.

ZnO	GGA-PBE	GGA-EV	Other cal.	Exp.values
WZ	0.783	1.80	0.98[35],0.80[36] 0.81[37]	3.44[40]
ZB	0.624	1.532	0.65[20], 0.64[27] 0.71[38]	3.27[39]

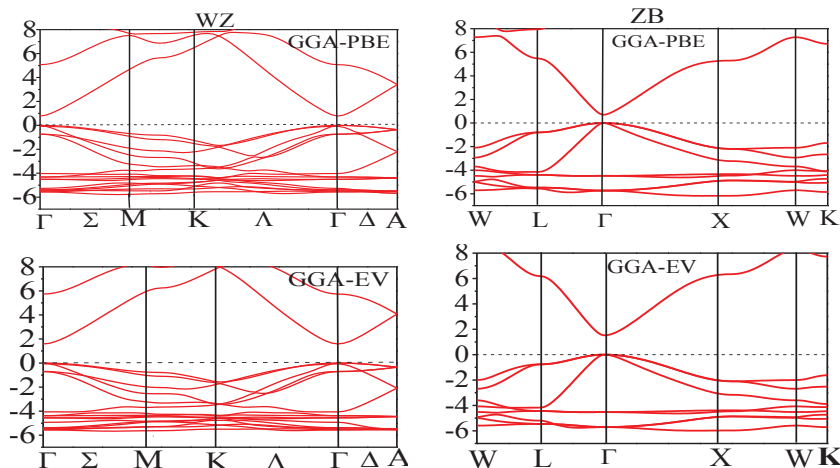


Fig. 2. Band structures of WZ, ZB of ZnO phases according to GGA-PBE and GGA-EV exchange correlation potentials.

Total density of states (DOS) results calculated for WZ and ZB of ZnO phases with GGA-PBE and GGA-EV are shown in Fig.3. Since the total and partial DOS profiles are similar for GGA-PBE and GGA-EV. The schematic representation of the total and partial DOS calculated using GGA-EV shows that the VB for ZnO is mostly dominated by Zn-d and O-p states. For the WZ phase the bands ranging from  $-6.6$  to  $-4$  eV are due to the Zn-3d states, whereas the O-2p states lie in the range from  $-5.941$  to  $0$  eV. For the ZB phase, Zn-d and O-p states appear in the energy range from  $-5.96$  to  $0$  eV, with maximum intensity at  $-5.55$  and  $-1.49$  eV, respectively. The two phases exhibit similar crystal symmetry and hybridization of states, with Zn atoms tetrahedral coordinated to O atoms. Both structural systems have strong hybridization of Zn-d and O-p states at the  $\Gamma$  point in the BZ, which causes coulomb repulsion and pushes the VB in the vicinity of Fermi level, and thus results in band gap narrowing [29].

### 3.3. Optical properties

#### Dielectric function

Among the most important parameter in an optical study, we can notice the dielectric function of the system. It is a complex quantity given as an addition of the real part  $\epsilon_1(\omega)$  and the imaginary part  $\epsilon_2(\omega)$  given by the following equation [30]:  $\epsilon(\omega) = \epsilon_1(\omega) + i\epsilon_2(\omega)$ .  $\epsilon_2(\omega)$  is directly related to the electronic band structure [45] and can be derived from the momentum matrix elements between the occupied and unoccupied electronic states, while  $\epsilon_1(\omega)$  can be obtained from  $\epsilon_2(\omega)$  using the Kramer–Kronig transformation [31]. A schematic over view of the dispersive part  $\epsilon_1(\omega)$  and the absorptive part  $\epsilon_2(\omega)$  for the tow ZnO phases calculated using GGA-PBE and GGA-EV are shown in Fig. 4. A shift in the absorption edge for  $\epsilon_2(\omega)$  towards higher energy is evident for GGA-EV compared to GGA-PBE.

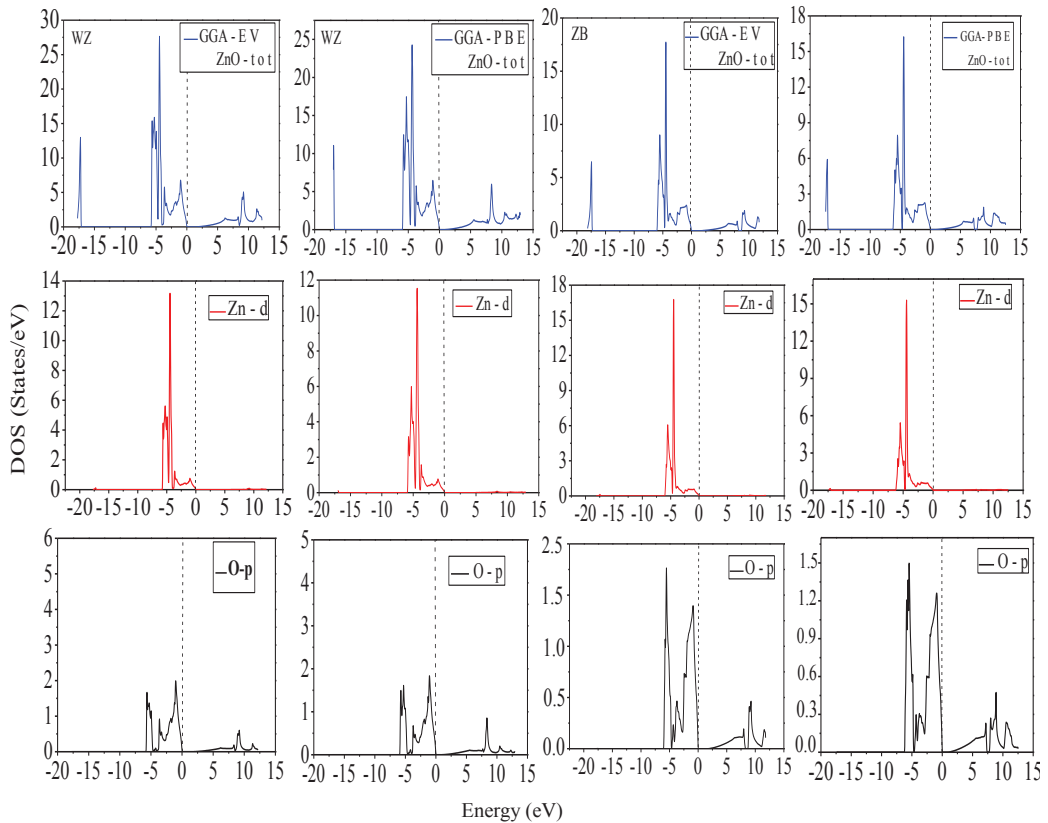


Fig. 3. Total and partial density of states for WZ, ZB of ZnO phases according to GGA-PBE and GGA-EV exchange correlation potentials.

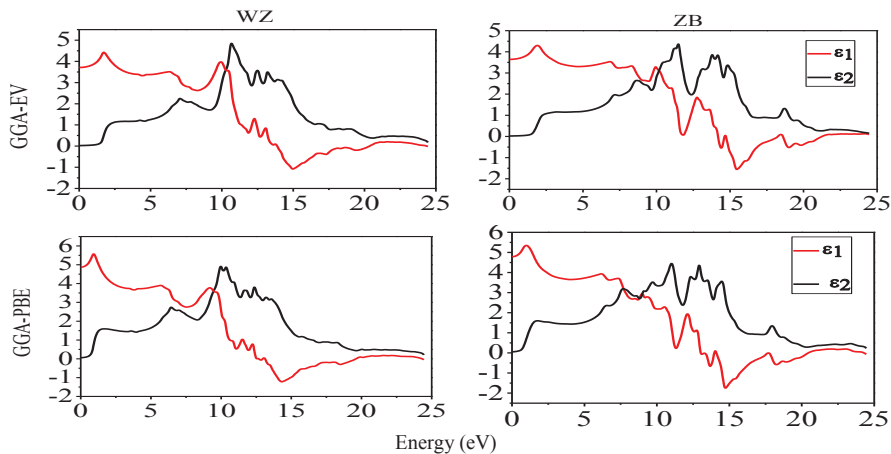


Fig. 4. Dielectric function for WZ and ZB of ZnO phases according to GGA-PBE, GGA-EV exchange correlation potentials. The black and red lines represent the imaginary and real parts of the dielectric function.

This is in agreement with the electric transition theory of the dielectric response, according to which the low energy edge of  $\epsilon_2(\omega)$  is related to the selection rules for electron transition in an optical one-photon process. The starting point for the optical absorption edge should be at least greater than the energy gap of the electronic

structure [32] for photo electron- induced transition between occupied and unoccupied states. Since the dielectric function results obtained with GGA-PBE and GGA-EV are qualitatively similar. For the WZ phase,  $\epsilon_2(\omega)$  exhibits three major peaks at 2.82, 7.06 and 10.65 eV (Fig. 4.black lines). These peaks were at 1.52, 6.47 and 10.02 eV GGA-PBE pseudo-potential calculations. The first and third peaks originate from direct optical transition of electrons between Zn-4s and O-2p and between O-2s and Zn-3d states, respectively. The second peak may be due to electron transition between O-2p and Zn-3d states. Peaks for the ZB phase can mainly be attributed to electron transition between O-2p and Zn-3d states. The Fig. 4 with red lines represents the real part of the dielectric function  $\epsilon_1(\omega)$ , which has three major peaks for the WZ phase at 1.71, 6.47 and 9.93 eV. However, these peaks are at 0.93, 5.75 and 9.28 eV according to GGA-PBE. Moreover, the three peaks are more intense for GGA-EV than GGA-PBE results. There is a steep decrease in  $\epsilon_1(\omega)$  intensity after the third peak and the parameter reaches zero at 13.84 and 12.54 eV for GGA-EV and GGA-PBE, respectively. After reaching a minimum value at 15.01 and 14.30 eV for GGA-EV and GGA-PBE, respectively, the intensity of  $\epsilon_1(\omega)$  again starts to increase with energy. Furthermore, the peaks for  $\epsilon_1(\omega)$  correspond to troughs for  $\epsilon_2(\omega)$ .

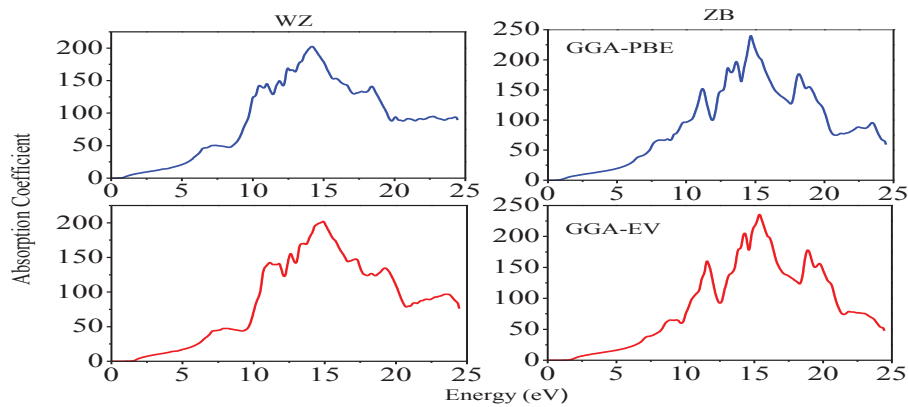


Fig. 5. Absorption coefficient for WZ and ZB phases according to GGA-PBE, GAA-EV exchange correlation potentials.

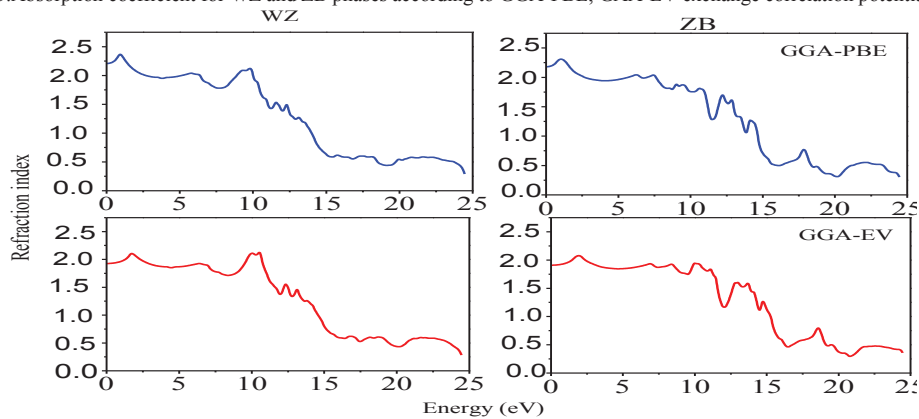


Fig. 6. Refraction index for WZ and ZB phases according to GGA-PBE, GAA-EV exchange correlation potentials.

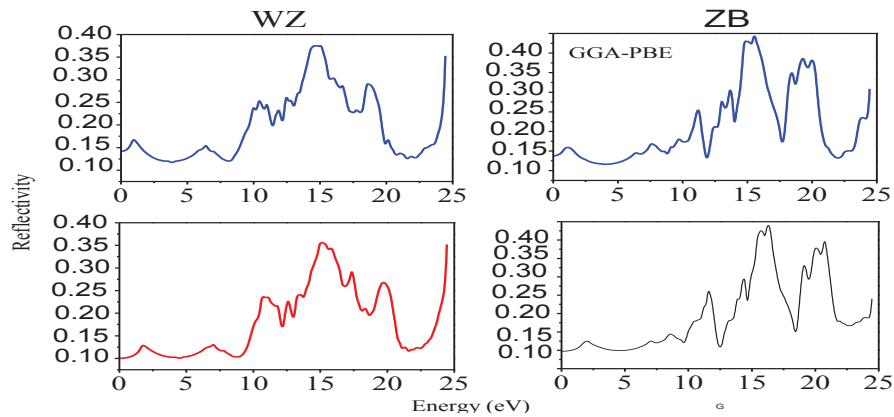


Fig. 7. Reflectivity for WZ and ZB phases according to GGA-PBE, GGA-EV exchange correlation potentials.

Other optical parameters such as absorption coefficient  $\alpha(\omega)$ , refractive index  $n(\omega)$  and reflectivity  $R(\omega)$  [43]. For optical devices, the absorption coefficient  $\alpha(\omega)$  is important. We first discuss  $\alpha$  and then discuss the other constants. From Fig.5. we can see the absorption coefficient of ZnO the major peak in the GGA-EV absorption spectrum for WZ is at 14.38 eV. However, in the GGA-PBE spectra it occurs at lower energy of and 14.12 eV. For ZB this peaks are in 15.40, 14.69 eV respectively. The optical absorption mainly originates from inter band electron excitation between the valence and the conduction bands. All of the absorption peaks can be corresponded to the peaks of  $\epsilon_2(\omega)$  spectra for GGA-EV and GGA-PBE in WZ and ZB phases deduced from the same electron transition. E.g. the first absorption peak corresponding to the first peak of  $\epsilon_2(\omega)$  spectra, deduced from the direct electron transitions from the O-2p states in valence band to the Zn-4s states in conduction band. The other optical constants are also important in designing optical devices. For example, the refraction  $n(\omega)$  and reflectivity  $R(\omega)$  shows in Fig.6. and Fig.7. respectively. When the energy is equal to zero, in WZ the refractive index  $n_0$  is 1.93 and 2.20 eV, and the reflectivity  $R_0$  is 0.10 and 0.14 eV for GGA-EV, and GGA-PBE, respectively. In ZB are  $n_0$  (1.91, 2.19eV),  $R_0$  (0.098, 0.13eV), respectively. The peaks of  $n(\omega)$  and  $R(\omega)$  can be observed in the curves, which are corresponding to the ones in  $\epsilon_2(\omega)$ , respectively.

#### 4. Conclusion

We studied the electronic and optical properties of WZ and ZB ZnO phases using GGA-PBE and GGA-EV for optical properties. The GGA-EV scheme yielded a wider VB and a narrower d band compared to the GGA-PBE results. The greater separation between O-p and Zn-d bands according to GGA-EV reduces the p-d repulsion and thus results in a wider band gap than GGA-PBE and is more consistent with experimental measurements. Optical properties calculated using GGA-EV was also in good agreement with experimental data and the results were better than for GGA-PBE. Our GGA-EV results for electronic properties are better in comparison to GGA-PBE; improvements in the XC functional are required for reliable results in DFT-based approaches for excited-state properties. Although GGA-EV results for optical properties are better in comparison to GGA-PBE.

## References

- [1] R. Ondo-Ndong, G.Ferblantier, M.AIKalfioui, A.Boyer, A.Foucaran, J.Cryst.Growth 255(2003)130.
- [2] Y.F.Gao, M. Nagai, Y.Masuda, F.Sato, K.Koumoto, J.Cryst. Growth 286 (2006)445.
- [3] A.P.chatterjee, P.M.Mitra, A.K.Mukhopadhyay, J.Mater.Sci.34 (1999)4225.
- [4] T.Minami, Semicond. Sci. Technol. 20(2005)35.
- [5] S.Saleh, H.Elsimary, A.Zaki, S.Ahmed, WSEAS Trans.Electron. 3(2006)192.
- [6] T.Minami, T.Miyata, K.Ihara, Y.Minamino, S.Tsukada, ThinSolid Films 494 (2006) 47.
- [7] P. Hohenberg, W. Kohn, Phys. Rev. B 136 (1964) 684.
- [8] W. Kohn, L.J. Sham, Phys. Rev. 140 (1965) A1133.
- [9] J.P. Perdew, Y. Wang, Phys. Rev. B 45 (1992) 244.
- [10] J.P. Perdew, K. Burke, M. Ernzerhof, Phys. Rev. Lett. 77 (1996) 3865.
- [11] J.P. Perdew, K. Burke, M. Ernzerhof, Phys. Rev. Lett. 78 (1997) 1396.
- [12] F. Tran, P. Blaha, Phys. Rev. Lett. 102 (2009) 226401.
- [13] V.I. Anisimov, J. Zaanen, O.K. Andersen, Phys. Rev. B 44 (1991) 943.
- [14] M.V. Ganduglia-Pirovano, A. Hofmann, J. Sauer, Surf. Sci. Rep. 62 (2007) 219.
- [15] D. Koller, F. Tran, P. Blaha, Phys. Rev. B 83 (2011) 195134.
- [16] L.J. Sham, M. Schluter, Phys. Rev. Lett. 51 (1983) 1888.
- [17] E. Engel, S.H. Vosko, Phys. Rev. B 47 (1993) 13164.
- [18] P. Dufek, P. Blaha, K. Schwarz, Phys. Rev. B 50 (1994) 7279.
- [19] Z. Charifi, H. Baaziz, A.H. Reshak, Phys. Stat. Solidi b 244 (2007) 3154.
- [20] A. Ashrfazi, C. Jagadish J. Appl. Phys. 102 (2007) 071101.
- [21] A. Segura, J.A. Sans, F.J. Manjon, A. Munoz, M.J. Herrera-Cabrera, Appl. Phys. Lett. 83 (2003) 278.
- [22] J.A. Sans, A. Segura, F.J. Manjon, B. Mari, A. Munoz, M.J. Herrera- Cabrera, Microelectron. J. 36 (2005) 928.
- [23] H. Karzel, W. Potzel, M. Köfferlein, W. Schiessl, M. Steiner, U. Hiller, G.M. Kalvius, D.W. Mitchell, T.P. Das, P. Blaha, K. Schwarz, M. P. Pasternak, Phys. Rev. B 53 (1996) 11425.
- [24] P. Blaha, et al., Wien2k, in: K. Schwarz (Ed.), An Augmented Plane Wave Plus Local Orbital Program for Calculating the Crystal PropertiesVienna University of Technology, Austria, 2001.
- [25] F. D. Murnaghan, Proc. Nat. Acad. Sci. U.S.A. 30 (1944)244.
- [27] A. Schleife, F. Fuchs, J. Furthmuller, F. Bechstedt, Phys. Rev. B 73 (2006) 245212.
- [28] S.H. Wei, A. Zunger, Phys. Rev. B 37 (1988) 8958.
- [29] X.B. Chen, L. Qi, M.Z. Ma, Q. Jing, G. Li, W.K. Wang, R.P. Liu, Solid State Commun. 145 (2008) 267.
- [30] J.S. Tell, Phys. Rev. 104 (1956) 1760.
- [31] H. Tributsch, Z. Naturf.A32 A (1977) 972.
- [32] R. Chowdhury, S.Adhikari, P.Rees, Physica B405 (2010) 4763.
- [33] U.Ozgurmetal., J. Appl. Phys. 98,041301 (2005)
- [34] S. Desgreniers, Phys. Rev. B 58 (1998) 14102 5
- [35] S.X.Cui, W.X.Feng, H.Q.Hu, Z.B.Feng, Y.X.Wang, J.AlloysCmpds.476(2009)306
- [36] B.Amrani, I.Chiboub, S.Hiadi, T.Benmessabih, N.Hamdadou,SolidStateCommun.137 (2006)395.
- [37] U.H.Bakhtiar et al. /Materials Science in Semi-conductor Processing 16(2013)1162– 1169
- [38] Y.Z.Zhu, G.D.Chen, H.G.Ye, Phys.Rev.B77 (2008)245209.
- [39] A.Ashrafi, A.Ueta, H.Kumano, I.Suemune, J.Cryst.Growth 221(2000)435
- [40] A.Mang, K.Reimann, S.Rubenacke, Solid State Commun.94 (1995)251.
- [41] G.M.Kalvius, D.W.Mitchell, T.P.Das, P.Blaha, K.Schwarz, M.P.Pasternak, Phys.Rev.B53 (1996)11425.
- [42] F.S.Decremp, F.Datchi, A.M.Saitta, A.Polian, S.Pascarelli, A.DiCicco,P.Iti.e. J.F.Baudelet,Phys.Rev.B68(2003)104101.
- [43] S. Saha, T.P. Sinha, A. Mookerjee, Physical Review B: Condensed Matter 62 (2000) 8828.
- [44] J.G. Lu, S. Fujita, T. Kawaharamura, H. Nishinaka, Y. Kamada, T. Ohshima, Z.Z. Ye, Y.J. Zeng, Y.Z. Zhang, L.P. Zhu, H.P. He, B. H. Zhao, J. Appl. Phys. 101 (2007) 083705.
- [45] Y.G.Zhang,G.B.Zhang,Y.X.Wang,J.Appl.Phys.109(2011)063510.